Experimental Investigation of the Effects of Base Mass Addition on the Near Wake of a Slender Body

JOHN E. LEWIS,* WILHELM BEHRENS,† AND DONALD J. COLLINS‡
TRW Systems, Redondo Beach, Calif.

The near wake of a two-dimensional wedge was studied at Mach 4. Static pressure, Pitot pressure, total temperature, injectant concentration and hot-wire fluctuations were measured. Helium, argon, and SF_6 were injected into the base, and their diffusion in laminar and turbulent wakes was studied. The locations of the wake stagnation points as a function of injection rate, and the critical rates required to eliminate the recirculating flow were determined. It was found that the near-wake flow with injection does not scale with the mass flux, nor do the momentum or the volume fluxes serve to correlate the data over the entire range of injection. Fluctuation measurements show that SF_6 has a destablizing effect on the wake, whereas helium has a stabilizing influence, compared to the wake without injection. Model cooling ($T_w/T_{0\infty} = 0.25$) resulted in a forward shift of the rear stagnation point and a pronounced decrease in both the velocity defect and the wake width but had a lesser effect on the distribution of the injected species.

Nomenclature

A = area of base of model (height of base × width over which gas was injected)
b = wake width
C_i = mass fraction, $C_i = \rho_i/\rho$
D = mass diffusion coefficient
f = frequency
H = base height
$\dot{I}$ = momentum flux parameter, $\dot{I} = \dot{M}_{BL}(\eta \text{air}/\eta i)^{1/2}$
$\dot{m}$ = mass addition, g/sec
$\dot{m}_{BL}$ = mass in model boundary layer $\int_0^\delta \rho u dy \cdot w$
M = Mach number
$\dot{M}_f$ = normalized mass addition, $\dot{M}_f = \dot{m}/\rho_\infty u_\infty A$
$\dot{M}_{BL}$ = normalized mass addition, $\dot{M}_{BL} = m/2\dot{m}_{BL}$
p = static pressure
Re_H = Reynolds number based on base height H and freestream conditions
S = Strouhal number, $S = fb/u$
Sc = Schmidt number, $Sc = \mu/\rho D$
T = static temperature
T_0 = total temperature
u = axial velocity
Δu = wake velocity defect, $u_e - u_\text{¢}$
W = width of model
x = streamwise distance aft of base
y = distance from wake centerline normal to freestream
γ = ratio of specific heats, $\gamma = c_p/c_v$
δ = model boundary-layer thickness
η = molecular weight
ρ = density
μ = viscosity

Subscripts

$(\ )_b$ = model base
$(\ )_\text{¢}$ = wake centerline
$(\ )_i$ = injection
$(\ )_{inj}$ = injection
$(\ )_\infty$ = freestream
$(\ )_e$ = wake edge
$(\ )_{SP}$ = stagnation point

Presented as Paper 70-110 at the AIAA 8th Aerospace Science Meeting, New York, January 19–21, 1970; submitted March 16, 1970; revision received April 23, 1971. This research was supported by the Advanced Research Projects Agency under Contract F04701-69-C-0119 and monitored by SAMSO, Norton Air Force Base, San Bernardino, Calif. The authors gratefully acknowledge the cooperation of NASA and the JPL wind-tunnel staff.

Index Categories: Supersonic and Hypersonic Flow; Jets, Wakes, and Viscid-Inviscid Flow Interactions.

* Manager, Engineering Technology Department, Fluid Mechanics Laboratory.

† Consultant to TRW; also Assistant Professor of Aeronautics, California Institute of Technology, Pasadena, Calif. Member AIAA.

‡ Consultant to TRW; also Research Fellow, California Institute of Technology, Pasadena, Calif. Member AIAA.

1. Introduction

NUMEROUS experimental and analytical studies of the supersonic wake have been made in the past few years. Recently, attention has been focused on the effects associated with mass addition. A number of important experimental studies have been made beginning with the works of Mohlenhoff,[1] Kingsland,[2] and Herzog,[3] and followed more recently by the works of Fox et al.,[4] Bauer,[5] Chapkis et al.,[6] Lewis and Chapkis,[7] Lewis and Behrens,[8] and Collins et al.[9] Although some aspects of the phenomena have been well defined by these investigations, many areas require further study. The works previously mentioned were all performed with adiabatic models and with injectants no heavier than argon.

The present experimental investigation has as its objective the determination of the behavior of the near-wake flowfield with base mass addition, with emphasis on the effect of injectants of large molecular weight and on the influence of model cooling.

A description of the behavior of the flowfield with mass transfer and the determination of the critical rate, beyond which no recirculation zone occurs in the flow, are discussed. The diffusion of the injected species for both laminar and turbulent wakes are considered, with particular attention given to the behavior of sulfur hexafluoride (SF_6) as an injectant. The behavior of the near wake under both adiabatic and cold wall ($T_w/T_{0\infty} = 0.25$) conditions with and without injection is studied. Finally, the effects of base mass addition on the stability of the near wake are discussed, with particular attention given to the contrast between sulfur hexafluoride and helium mass addition.

2. Experimental Procedure

The experiments were performed in the supersonic wind tunnel of the Jet Propulsion Lab., Pasadena, Calif., which is

an 18 × 20-in. continuous flow facility. The study was made at Mach 4.0 and over a range of Reynolds numbers yielding both laminar and turbulent wakes ($Re_H = 2.7 \times 10^4 \rightarrow 1.6 \times 10^5$).

The model used for this study is a two-dimensional 6°-half angle wedge of 1-in. base height, which spans the 18-in. wide tunnel. Fences large enough to contain the subsonic wake flow were mounted on the base (extending $6H$ downstream of base) just inside the wind-tunnel boundary layers in order to isolate the interaction with them (distance between fences/baseheight = 13). The resulting configuration is believed to approximate well a two-dimensional flow (see Batt and Kubota[10]). (A detailed description of the model can be found in Refs. 6 and 7.) The model has a porous base from which helium, nitrogen, argon, and SF_6, whose molecular weight is five times that of air, were injected. Cold wall tests were conducted by cooling the model with liquid nitrogen, which resulted in a wall temperature $T_w/T_{0\infty} \cong 0.25$. Under the cold wall conditions, only helium could be used as an injectant because of the higher liquefaction temperatures of the other gases.

The Pitot pressure, static pressure, injectant mass fraction, hot-wire voltage fluctuations, and the total temperature were measured simultaneously using a five-probe rake, constructed to minimize probe interference.

Hot-wire fluctuation measurements (f = 1–160 KHz) were used to determine the laminar or turbulent state of the wake, the relative growth or decay of fluctuations, and their energy spectra. These measurements were made at high enough overheats so that for the adiabatic configuration, the signals are essentially proportional to the mass flow fluctuations, $\overline{(m'/\bar{m})^2}$.

The static pressure was measured across the wake but little variation was detected, and the data was reduced using a constant mean value. The injectant mass fraction $C_i = \rho_i/\rho$ was measured by the use of an aspirating probe in conjunction with a mass spectrometer for which a calibration was obtained from controlled samples of each of the gases used in the experiment. This system is identical to that described in detail by one of the authors in Ref. 9. The aspirating probe obtains a sample representative of the undisturbed flowfield even for the reversed flow region.[9]

Using the measured mass concentration, the specific heat ratio γ was determined from the equation

$$\gamma = \gamma_{air} \frac{1 + \{(\gamma_i/\gamma_{air})[(\gamma_{air} - 1)/(\gamma_i - 1)]\eta_{air}/\eta_i - 1\}C_i}{1 + \{[(\gamma_{air} - 1)/(\gamma_i - 1)]\eta_{air}/\eta_i - 1\}C_i}$$

where for helium and argon, $\gamma_i = 1.67$. However, for SF_6, γ is a strong function of temperature even at room temperature.[11] Therefore, for SF_6 injection, γ and temperature must be calculated by iteration. For the cold wall model, the total temperature was inferred from the recovery temperature of a cylinder probe described in Ref. 12. For the adiabatic model tests, the variation in total temperature was neglected.

Finally, in order to insure that the data presented was self-consistent, the injectant mass balance was checked by comparing

$$\dot{m}_i = \int_{-\infty}^{\infty} \rho_i u dy$$

with the injected mass flow monitored by a calibrated meter during the test. At the furthest downstream stations (X/H = 8,15), some three-dimensional effects are present. The data presented have mass balance deviations of typically 25%.

A special probe was used to determine stagnation points in the wake. Following Batt and Kubota,[10] the pressure difference between the stagnation point and the base of a small cylinder (d = 0.080 in.) was measured using a U-tube silicone manometer.

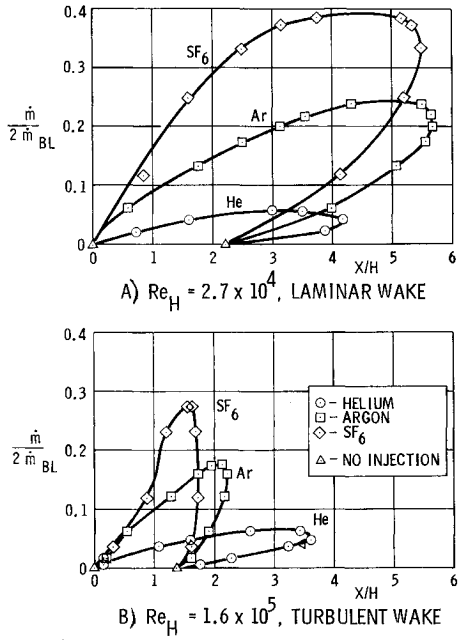

Fig. 1 Near-wake stagnation point locations with base mass addition.

3. Effect of Injection on Recirculating Flow

Rear Stagnation Point Location without Injection

In order to assess the effect of base injection on the base flow region, the stagnation points were mapped as a function of axial position using the special stagnation probe previously described. For no base injection the rear stagnation point in the near wake at hypersonic Mach numbers is known to occur at $(X/H)_{SP} \cong 0.8$ independent of Reynolds number, wake transition, and wall temperature.[10,13] For the present study at Mach 4, however, we find the stagnation point of the laminar adiabatic wake ($Re_H = 2.7 \times 10^4$) to occur at $(X/H)_{SP} = 2.2$, and at this Mach number wake transition

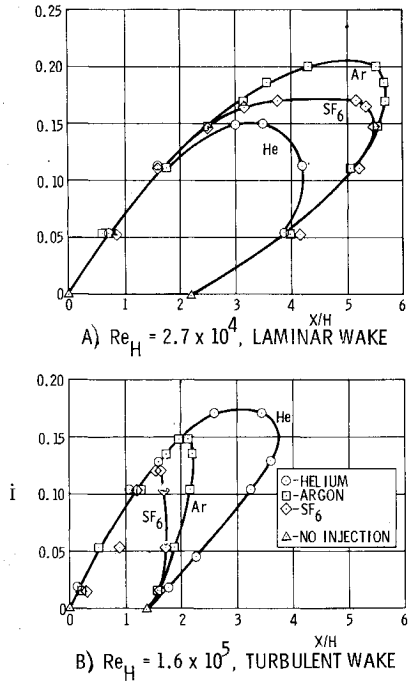

Fig. 2 Momentum flux scaling of stagnation point locations with base mass addition.

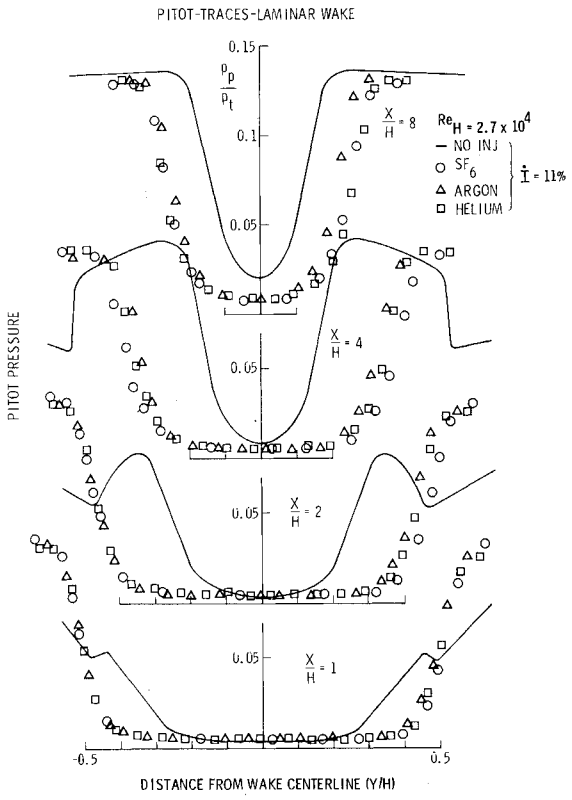

Fig. 3 Near-wake Pitot profiles—matched momentum flux $\dot{I}$ (laminar wake).

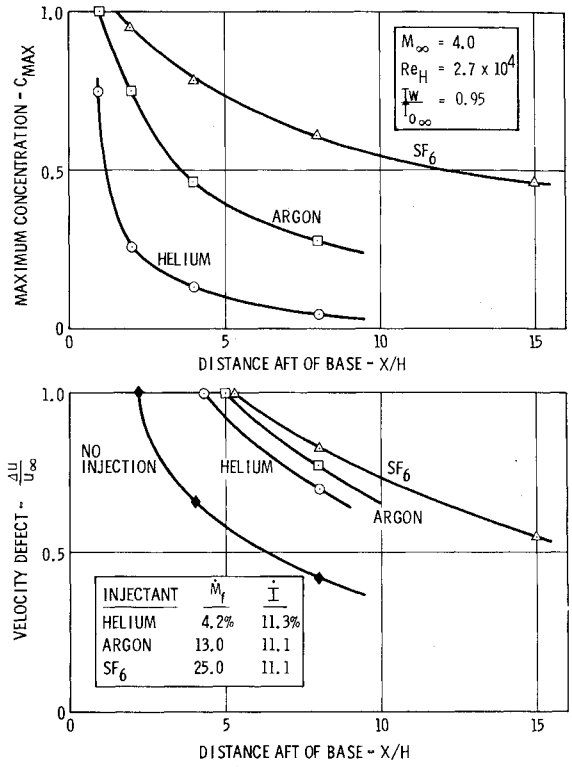

Fig. 5 Maximum concentration and velocity defect—laminar wake, low injection rate.

and wall cooling have a large effect on its location. As the Reynolds number is increased to 1.6×10^5, transition moves to the neck and $(X/H)_{SP} \simeq 1.4$. At $Re_H = 3.2 \times 10^5$, transition occurs at the base of the wedge and $(X/H)_{SP} \simeq 0.6$. Tripping the boundary layer at this Reynolds number results in $(X/H)_{SP} \cong 0.8$. When the model was cooled ($T_w/T_{0\infty} = 0.25$), the stagnation point occurred at $(X/H)_{SP} = 1.2 \pm 0.2$§ for both the laminar and the turbulent wakes.

Hence, for the laminar, adiabatic wake, the rear stagnation point is found to move aft with decreasing Mach number; however, the effect of cooling and/or turbulence reduces the extent of the recirculating flow. These apparently new stagnation point results are further substantiated by Hama's shadowgraphs, as shown in Ref. 8 (Figs. 2 and 7). Note also that in the laminar near wake of a cone at $M_\infty = 4.3$ and $Re_D = 4 \times 10^4$, McLaughlin[14] measured a rear stagnation point location of $(X/D)_{SP} = 2.5 \pm 0.5$.

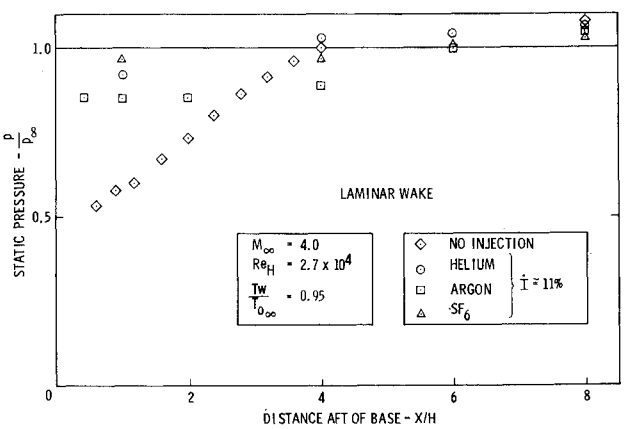

Fig. 4 Wake centerline static pressure distribution.

Stagnation Points and Near-Wake Flow with Base Injection

For small rates of base injection, the recirculation region detaches from the base of the body and forms a bubble with two stagnation points on the axis. Beyond some critical injection rate there is no stagnation point in the flow. This rate is commonly referred to as a blow off rate; however, as pointed out in Ref. 7, the recirculating bubble does not continue to move downstream but instead shrinks to a single stagnation point at the critical rate. In Fig. 1, the stagnation point locations are plotted as a function of the injected mass. Both the laminar and the turbulent wake show that for a given mass flow, the effect of helium is much greater than that of the heavier gases.

For the laminar wake with low injection rates, the changes in the over-all flowfield are best correlated with the momentum flux parameter $\dot{I}$ as found earlier.[9] This is evidenced both in the stagnation point locations given in Fig. 2, and in the Pitot and static-pressure distributions shown in Figs. 3 and 4. For the laminar wake at higher injection rates and for the turbulent wake at all injection rates, this scaling does not hold. The maximum downstream locations of the stagnation points show that the data can never be exactly collapsed by a simple scaling of the injectant, e.g., volume or momentum flux. The differences are more pronounced for the turbulent wake (the model boundary layers are laminar) because of the effect of the injectant on wake transition.

Finally, it is important to note that while no stagnation point exists for $\dot{I} \gtrsim 0.2$, there is an extensive region of very low-speed flow in the wake for even larger rates. The major difference between sub- and super-critical injection is seen in the concentration profiles discussed in the following section.

§ For the cold model, the location of the stagnation point was inferred from the Pitot-static differential pressure and is not as accurate as the results obtained with the stagnation point probe.

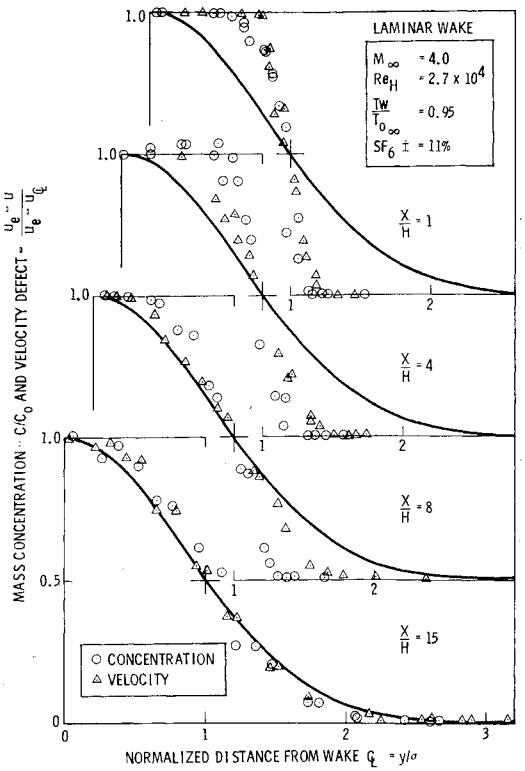

Fig. 6 Concentration and velocity profiles—laminar wake, SF_6 injection (low injection rate).

4. Diffusion

Laminar Near Wake with Low (Subcritical) Rate of Injection

At low injection rates in laminar wakes, the momentum flux $\dot{I}$ provided the best correlation of the over-all flowfield (stagnation point, wake thickness, shocks, etc.). Whereas these gross effects of the injection are adequately correlated with $\dot{I}$, the injectant mass fraction C_i and the detailed velocity distributions show significant differences. The decay of the maximum concentration,¶ C_{max} and the centerline velocity defect in the laminar wake for a single value of $\dot{I}$ for helium, argon, and SF_6 injection are plotted in Fig. 5 to illustrate the effect of the different diffusion coefficients. The much larger mutual diffusion coefficient of helium-air compared to that of SF_6-air is dramatically illustrated. The differences in the velocity defect measurements are less distinct.

Figure 6 shows the corresponding transverse distributions of the mass concentration, normalized with the centerline value, and the velocity defect $(u_e - u)/(u_e - u_\ell)$ for SF_6. The distributions for helium injection are similar and therefore are not shown. The γ coordinate has been normalized with the profile half width, and a Gaussian curve has been used as a reference, to illustrate the relaxation of the normalized profiles with increasing distance from the model.

Whereas the proper coordinate is the incompressible Howarth coordinate, it is remarkable that the velocity and mass concentration distributions rapidly approaches the Gaussian form in the physical plane, despite the differences illustrated at $X/H = 1$. The pronounced off-axis overshoot in the mass concentration exhibited by profile $X/H = 2$ is a direct consequence of the existence of reversed flow (see Fig. 1). In this case, low mass concentration fluid from the vicinity of the rear stagnation point is convected into the recirculating zone, depressing the centerline concentration below

¶ This is synonymous with the centerline concentration with the exception of measurements within regions of reverse flow.

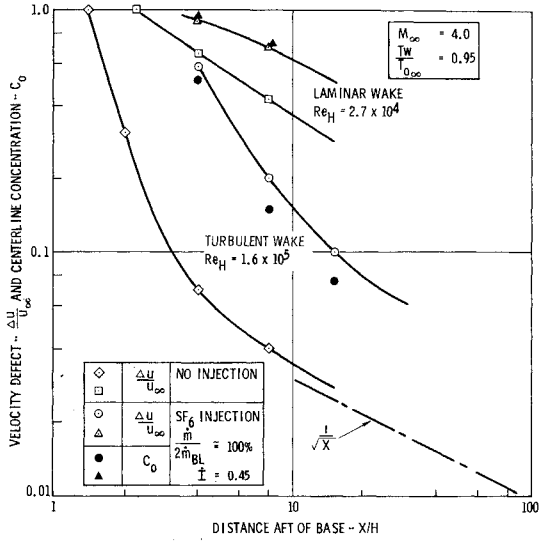

Fig. 7 Velocity defect—SF_6 injection.

the value that would exist in the absence of the reversed flow. Besides the off-axis overshoot in the concentration profiles in the recirculation zone, the velocity profiles and the concentration profiles are quite similar and are nearly equal in width (within 10%); in addition the static pressure is almost constant. These results should aid in the analytical modeling of the diffusion process.

Laminar and Turbulent Near Wakes with Supercritical Rate of Injection

In Fig. 7, the centerline velocity defect is plotted for both the no-injection case and for SF_6 injection rates equal to the boundary-layer mass flow ($\dot{I} \simeq 0.45$) for both the laminar and turbulent wake. The consequence of mass addition is to increase the centerline velocity defect at a given axial station over that existing in the absence of mass addition. This

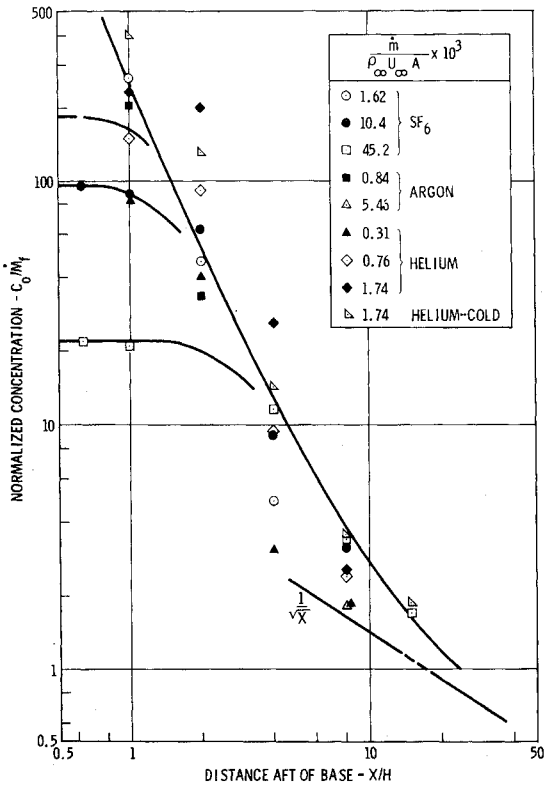

Fig. 8 Normalized concentration—turbulent wake.

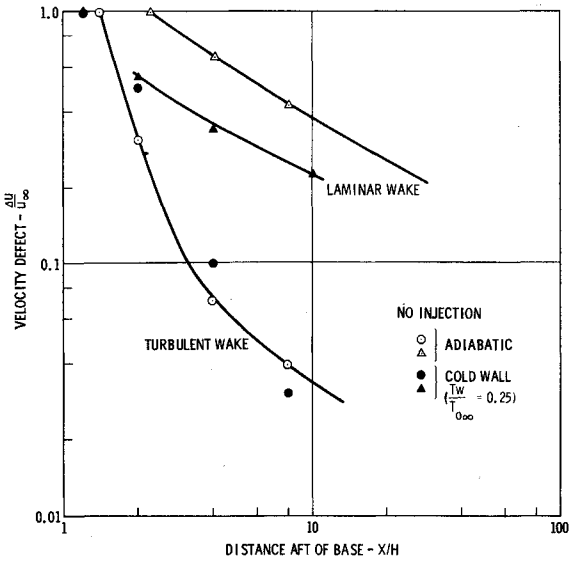

Fig. 9 Velocity defect with and without cooling.

effect is accentuated in the turbulent wake as a consequence of the existence of an initially laminar inner core and the subsequent transition in the vicinity of the neck. In Fig. 7, the SF_6 mass concentrations are also shown. The mass concentrations decay at the same rate as the velocity defect.

For both flows, the mass addition rate is sufficiently large that no recirculating zone exists in the near wake and $dp/dx \cong 0$. Hence, the diffusion of mass and momentum are governed by identical equations provided $Sc = \nu/D = 1$. For laminar flow, the Schmidt number for SF_6 is nearly unity. The results for the distribution of velocity defect and mass concentration are nearly identical. For the turbulent case, the mass concentrations are lower than the velocity defects, implying a turbulent Schmidt number slightly less than unity. It is concluded that for SF_6, an approximation of a unit turbulent Schmidt number is valid, whereas for helium-injection,

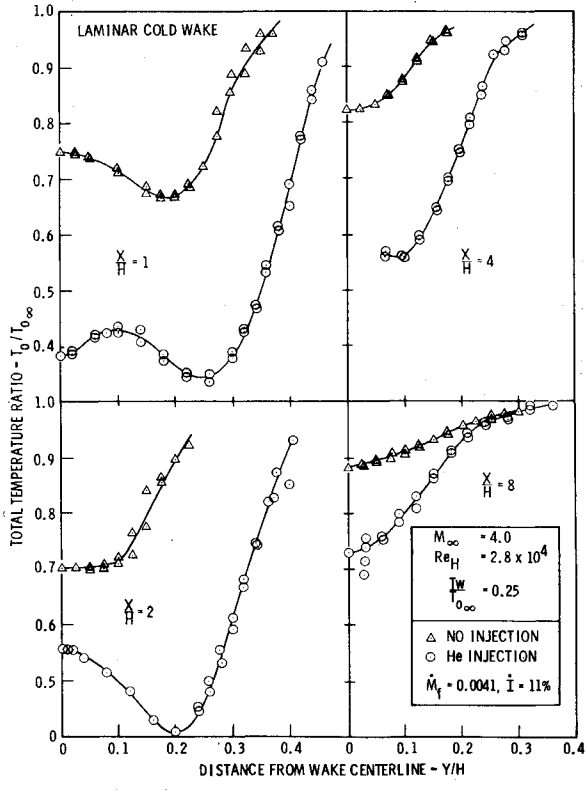

Fig. 10 Total temperature profiles—laminar wake.

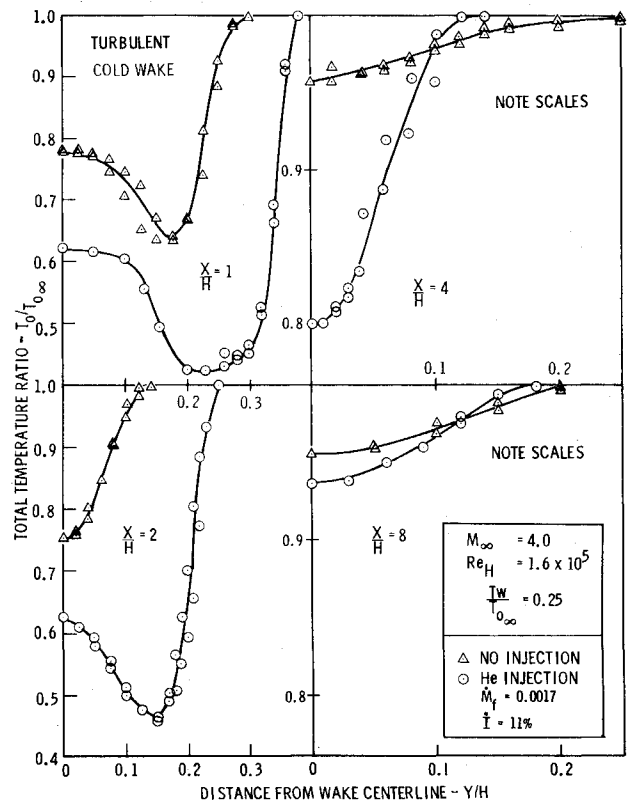

Fig. 11 Total temperature profiles—turbulent wake.

its effect is to decrease the turbulence level significantly (Sec. 6), giving a more characteristically laminar Schmidt number.

Measured concentration and velocity distributions for this supercritical rate of SF_6-injection (no recirculation region) into the laminar wake, are very similar to the profiles shown in Fig. 6 (except for the overshoot in concentration shown there off-axis at $X/H = 2$). For the case of the turbulent wake, the concentration and velocity profiles (in physical coordinates) are nearly Gaussian at $X/H = 4$, even though at $X/H = 1$ the profiles are top-hat profiles (see Fig. 6, $X/H = 1$).

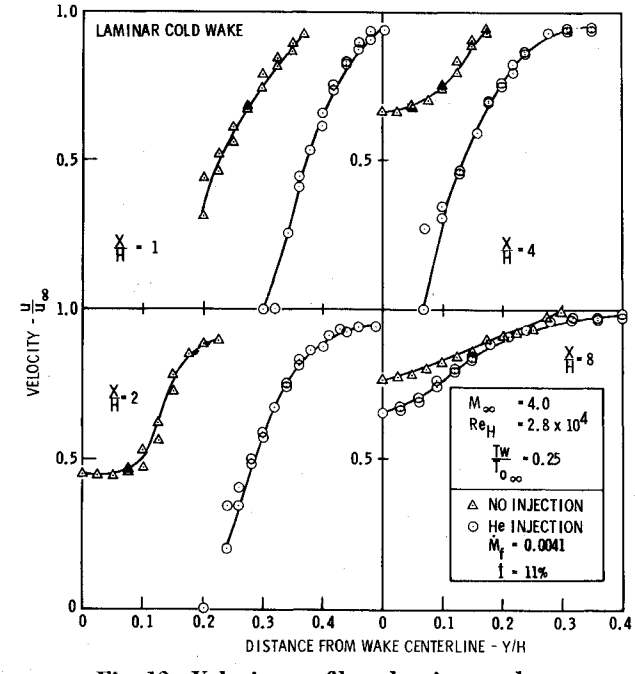

Fig. 12 Velocity profiles—laminar wake.

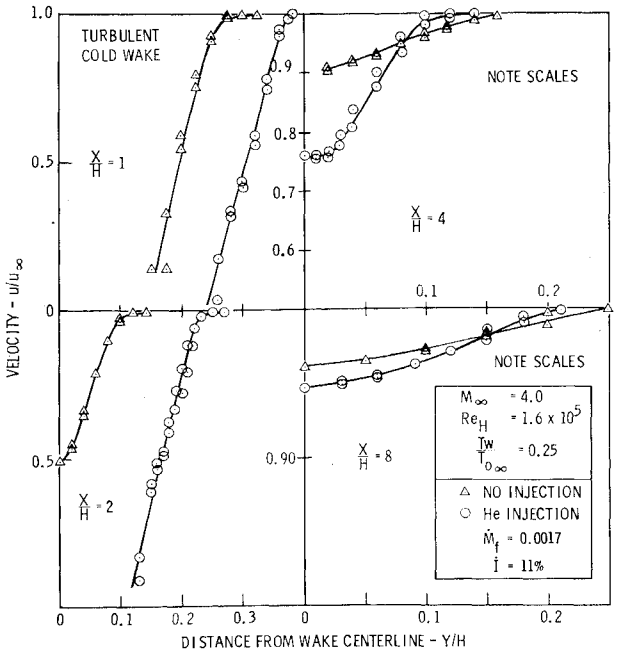

Fig. 13 Velocity profiles—turbulent wake.

Decay of Centerline Mass Concentrations in Turbulent Wakes

For the turbulent wake, the axial decay of mass concentration has been plotted in the Oseen variable $C_\ell/\dot{M}_f$ in Fig. 8 for all cases studied.[9] Although the values of C_ℓ vary as much as 100, we seen that when normalized with $\dot{M}_f$ (with the exception of the highest helium injection rate where some laminarization of the wake may be present) and away from the short initial region where $C_\ell/\dot{M}_f \rightarrow 1/\dot{M}_f$, the data coalesce to a single curve within a factor of 2. Better agreement might be obtained by transforming the data to the incompressible plane and properly accounting for a shift in the virtual origin.

For the majority of the cases presented, the effects of SF_6 condensation, if present, are believed to be second order, based on the amount of mass involved in the process. On the other hand, for $\dot{M}_{BL} = 1.0$ for the turbulent wake, the data at $X/H = 8,15$ would be affected to the greatest degree, and must be interpreted with caution.

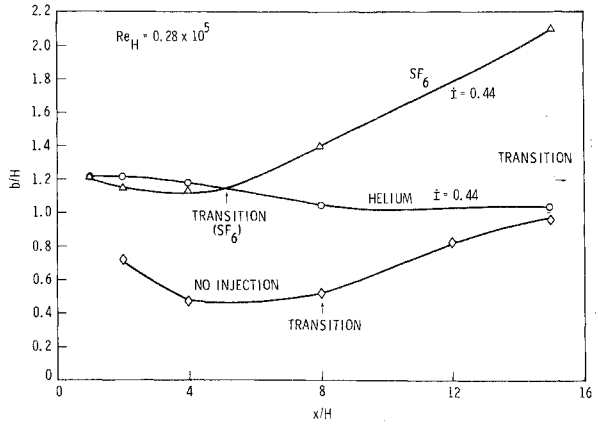

Fig. 14 Wake widths with and without injection.

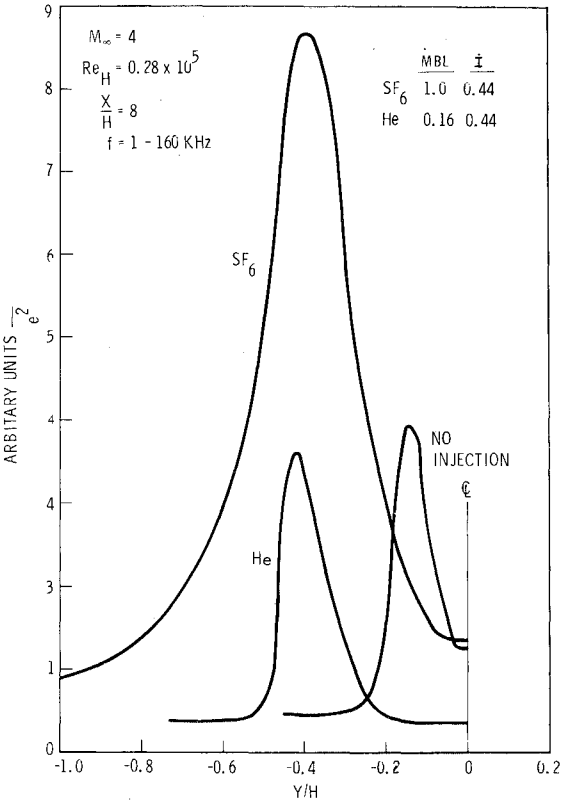

Fig. 15 Fluctuation intensity surveys.

5. Cooling

Cold Near Wake without Injection

The effect of model cooling on the near wake of a slender wedge, in the absence of base mass addition, has been investigated in detail by Batt and Kubota[10] at $M_\infty = 6$. For the

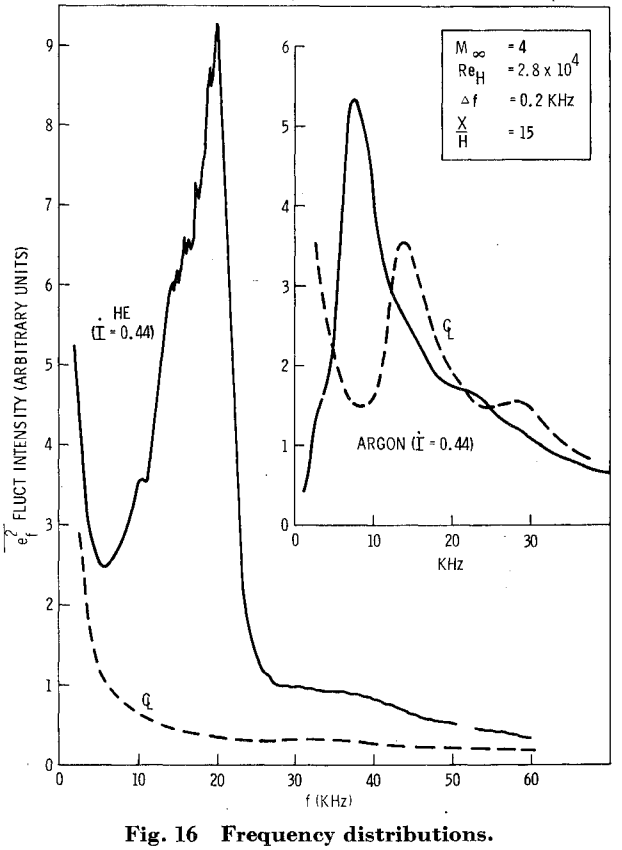

Fig. 16 Frequency distributions.

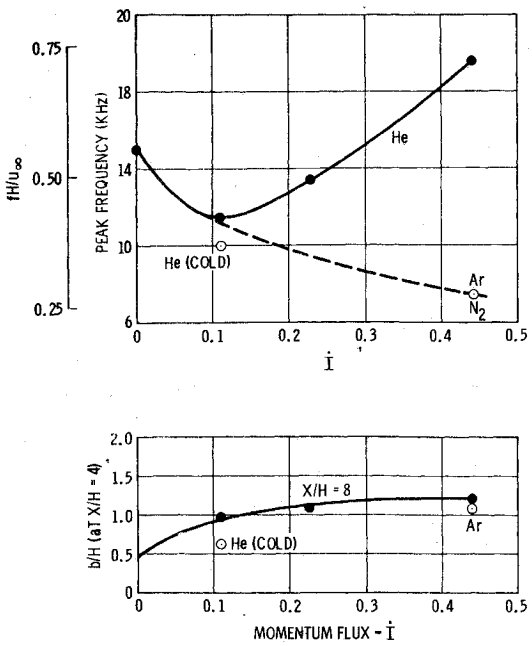

Fig. 17 Fundamental frequency of oscillations in wakes with injection.

purely laminar case, they observed a significant decrease in thickness of the free shear layers and the near wake. The effect on the location of the rear stagnation point and the velocity defect in the wake was found to be small. In the present investigation at $M_\infty = 4$ cooling ($T_w/T_{0\infty} = 0.25$) again decreased the scale of the near wake. For the laminar wake, the rear stagnation point moved from $(X/H)_{SP} = 2.2$ to $(X/H)_{SP} \simeq 1.2 \pm 0.2$ with cooling, the effect being much smaller for the turbulent wake. The velocity defect, $\Delta u/u_\infty$, has been plotted as a function of X/H for both the laminar and the turbulent no-injection wakes in Fig. 9, to illustrate the effect of cooling. The effect on the turbulent wake is seen to be small; however, the laminar wake velocities are considerably altered. The reason for this behavior is believed to be a direct result of the forward motion of the rear stagnation point which is, in essence, the origin of the velocity wake.

Total temperature profiles in the cold wakes are shown in Figs. 10 and 11. The most striking feature of these profiles is that the total temperature minimum is not always on the axis. For the no-injection wakes (laminar and turbulent) at $X/H = 1$, the minimum occurs near $Y/H \cong 0.2$. The mechanism responsible for this behavior is the convection into the recirculating zone of the high-temperature gas from the region near the rear stagnation point, which elevates the centerline total temperature above that which would exist in the absence of the recirculating flow. This is the same mechanism responsible for the structure of the mass concentration profiles within the recirculating zone. A second interesting feature of the wake without injection is that the minimum temperatures as close as $X/H = 0.5$ are $T_0/T_{0\infty} = 0.58$ and 0.62 for the laminar and turbulent cases, respectively. Since $T_w/T_{0\infty} = 0.25$, these results imply that there is a thin thermal layer near the base as suggested by Scott and Eckert.[14] This conclusion has to be kept in mind when interpreting the total temperature profiles with helium injection.

Cold Wake with Helium Injection

As in the adiabatic case with helium injection, the wake widens, the recirculation zone increases in length, and the shear layers are displaced outward, as evidenced by the comparisons of the total temperature profiles and the velocity profiles shown in Figs. 12 and 13. As can be seen, both the velocity and temperature distributions are considerably altered with base injection. A recirculation region still exists for these rates of injection and the off-axis minimum of total temperature is evident. For the laminar wake, two minima occur, and it is believed that this profile occurs near the forward stagnation point. The minimum total temperature at $X/H = 1$ is $T_0/T_{0\infty} = 0.33$ (laminar wake) and 0.43 (turbulent wake) as compared to $T_0/T_{0\infty} = 0.67, 0.64$ for the wakes without injection. Thus, the thin thermal layer on the base of the body is removed by injection, considerably decreasing the total temperature in the near wake.

The rate of diffusion of helium is changed very little by cooling, as found by comparison of the centerline concentrations for the adiabatic and cold cases. The concentration profiles in the cold wakes are qualitatively similar to the total temperature and velocity profiles.

Finally, a comparison of the adiabatic and the cooled wake with equal mass flows of helium injection ($\dot{M}_f = 0.0042$) shows that transition occurs much sooner in the case of the cooled wake. The onset of nonlinearity is $X/H = 6$ compared to $X/H = 10$ for the adiabatic wake. This result is in agreement with the observations of Ref. 10, in which wake transition was found to move upsteam with decreasing wall temperature.

6. Effect of Injection on Wake Stability

Hot-wire fluctuation traces ($f = 1$–160 KHz) were made across the wake with the energy spectrum measured at selected points in the wake. These measurements were then used to determine the laminar or turbulent state of the wake and to study the effect of the base mass addition on wake stability.

For the laminar wake ($Re_H = 2.7 \times 10^4$), and for $\dot{I} \cong 0.11$, the wake thickness, pressure distribution, and velocity distribution are approximately independent of the injectant. However, the mass concentrations, as pointed out previously, are quite different. Wake stability and transition are also found to be strong functions of the molecular weight of the injectant.

Without base injection, wake transition occurs at $X/H = 8$. Helium injection delays transition beyond the range of the measurements ($X/H \geq 15$). Injection of SF_6 hastens transition to $X/H \cong 5$. The growth of the wakes for the same $\dot{I}$ (Fig. 14) reflects the movement of the transition point. The hot-wire fluctuation surveys at $X/H = 8$ are shown in Fig. 15 for SF_6, helium and no injection, where the considerably increased turbulence level and wake width for the SF_6 injection are evident.

The energy spectra of fluctuations (Fig. 16) confirm that a wake with helium injection is still in the linear instability region. A very pronounced peak occurs in the frequency spectrum, and there is very little fluctuation energy on the wake axis. Argon and nitrogen injection result in a transition to a nonlinearly unstable wake at $X/H \simeq 10$. Energy spectra at the points of maximum signal for both of these gases are about the same and both exhibit a large peak at the same frequency. However, for argon injection, beyond $X/H = 10$, there is a much more pronounced harmonic on the wake axis than in the case of nitrogen injection. The energy distribution of fluctuations for the SF_6 wake at all stations is a broad-turbulent spectrum without any sign of a preferred frequency. Thus, for the case of SF_6 injection, the wake appears to become fully turbulent within five base heights without the occurrence of a periodicity in the unstable laminar wake.

The results of helium, argon and nitrogen injection are in agreement with the previous findings of Ref. 8, where base injection has found to stabilize the wake. The SF_6 injection clearly acts in the opposite way. The reason for this behavior is believed to be associated with the effect of density on the amplification rates. All base injection will have a stabilizing effect associated with the reduction of pressure gradients in the wake. Provided the density of the injectant is

less than that of air, the injection should always result in a delay in wake transition. However, for injectants which are heavier than air, the positive effect of base injection can be more than offset by the increased wake densities and may well hasten the onset of transition as was found in the present study with SF_6.

There are pronounced peaks in the frequency spectra in the wakes without injection and for helium and argon injection, indicating that in the laminar wakes there is a relatively narrow range of very unstable frequencies. It has been found that in laminar wakes of slender bodies both at hypersonic and at low speeds (incompressible), the most unstable frequency may be related to a characteristic laminar wake width and the freestream velocity (wake edge velocity). A nondimensional invariant, $S = f_{max}b/u_e \simeq 0.3$, was found by Behrens and Ko,[15] where b is the laminar wake width just downstream of the neck, which changes very little as long as the wake does not become nonlinearly unstable. This constant Strouhal number can be explained in terms of linear stability theory. In the wake without injection, $f_{max} \simeq 15$ KHz and $S \simeq 0.26$.

In the case of N_2 and argon injection, $f_{max} \simeq 7.5$ KHz, but the wake width is approximately twice as wide and $S = 0.275$ (N_2); $= 0.285$ (argon) in good agreement with the findings of Ref. 15. However, for helium injection, f_{max} does not decrease; it increases considerably ($f_{max} = 19.5$ KHz), even though the wake width increases by more than a factor of two. For all cases for which a dominant frequency was found, f_{max} and the wake width at $X/H = 4$ are plotted as functions of injection rate $\dot{I}$ in Fig. 17. In all cases of helium injection, the Strouhal number varies considerably. Note also, as the wake with helium injection is cooled by LN_2, the wake becomes narrow, but also the most unstable frequency decreases. From these measurements, it appears that the change in density profile caused by the helium injection not only delays transition but also has a pronounced effect on the value of the most unstable frequency.

7. Summary

An experimental study has been made of the effect of base mass addition on the near wake of a slender wedge at Mach 4. The important conclusions of this investigation are the following.

1) The rear stagnation point of the laminar, adiabatic wake is considerably further aft of the base at Mach 4 than the hypersonic value of 0.8. At this Mach number, cooling and the onset of near wake transition are found to have a strong effect on this location.

2) For the laminar wake with low injection rates, the changes in the over-all flowfield (stagnation points, wake thickness, shocks, etc.) are best correlated with the momentum flux. However, the concentration distributions reflect a strong dependence on the molecular weight of the injectant. Further, no simple scaling of the injectant can account for the differences in either the laminar or turbulent wake for higher rates of injection.

3) For $\dot{I} \gtrsim 0.2$, no stagnation point exists in the wake; however, there remains an extensive region of low-speed flow in the core of the wake for even larger injection rates.

4) Both mass concentration and total temperature profiles within the recirculation region show off-center maxima which are interpreted to be the result of the dominance of reverse flow convection over diffusion.

5) The result of base mass addition is to increase the velocity defect in the wake. This effect is accentuated in the turbulent wake due to an initially laminar core formed by the injectant.

6) In both laminar and turbulent wakes, the approximation of a unit Schmidt number is valid for SF_6 injection but not for helium injection.

7) For a turbulent wake, centerline concentrations when normalized with $\dot{M}_f$ are reasonably independent of injectant or rate of injection.

8) The laminar wake velocities (no injection) are considerably altered by model cooling as a result of the forward motion of the rear stagnation point, but the effect on the turbulent wake is small.

9) Helium injection under cold wall conditions results in greatly reduced total temperatures in the near wake compared to wakes without injection.

10) Wake transition moves upstream with decreasing wall temperature.

11) For injectants whose molecular weight is less than air, base injection results in a delay in wake transition. However, SF_6 injection can, and in the present study did, hasten the onset of transition.

12) For most wakes with and without base injection, the most unstable frequency can be characterized by a Strouhal number, $S = f_{max}b/u_e = 0.3$. Helium injection is found to be an exception.

References

[1] Mohlenhoff, W., "Experimental Study of Helium Diffusion in the Wake of a Circular Cylinder at M = 4.8," Memo 54, May 20, 1960, GALCIT Hypersonic Research Project, California Institute of Technology, Pasadena. Calif.

[2] Kingsland, L., Jr., "Experimental Study of Helium and Argon Diffusion in the Wake of a Circular Cylinder at M = 5.8," Memo 60, June 1, 1961, GALCIT Hypersonic Research Project.

[3] Herzog, R. T., "Nitrogen Injection into the Base Region of a Hypersonic Wake," Memo 71, Aug. 15, 1964, GALCIT Hypersonic Research Project.

[4] Fox, H., Zakkay, V., and Sinha, R., "A Review of Some Problems in Turbulent Mixing," Rept. NYU-AA-66-63, Sept. 1966, New York Univ.

[5] Bauer, A. B., "Effect of Vehicle and Fluid Injection Geometries on Near-Wake Flow Field Structure," Publication V-4028, Feb. 1967, Aeronutronic Div. of Philco-Ford, Newport Beach Calif.

[6] Chapkis, R. L., Fox, J., Hromas, L., and Lees, L., "An Experimental Investigation of Base Mass Injection on the Laminar Wake Behind a 6-Degree Half-Angle Wedge at M = 4.0," Rept. 06388-6009-R000, April 1967, TRW Systems, Redondo Beach, Calif.

[7] Lewis, J. E. and Chapkis, R. L., "Experimental Investigation of the Effect of Base Injection on the Near Wake of a Slender Wedge at Mach 4.0," *AIAA Journal*, Vol. 7, No. 5, May 1969, pp. 835–841.

[8] Lewis, J. E. and Behrens, W., "Fluctuation Measurements in the Near Wake of a Wedge with and without Base Injection," *AIAA Journal*, Vol. 7, No. 4, April 1969, pp. 664–670.

[9] Collins, D. S., Lees, L., and Roshko, A. I., "Near Wake of a Hypersonic Blunt Body with Mass Addition," *AIAA Journal*, Vol. 8, No. 5, May 1970, pp. 833–842.

[10] Batt, R. G. and Kubota, T., "Experimental Investigation of Laminar Near Wakes Behind 20° Wedges at $M_\infty = 6$," *AIAA Journal*, Vol. 6, No. 11, Nov. 1968, pp. 2077–2083.

[11] McBride, B. J., Heimel, S., Ehlers, J. G., and Gordon, S., *Thermodynamic Properties to 6000°K for 210 Substances Involving the First 18 Elements*, SP-3001, NASA, 1963.

[12] Behrens, W., "Total Temperature Probe Based on Recovery Temperature of a Circular Cylinder," Internal Memo 18, May 1969, GALCIT Hypersonic Research Project; *International Journal of Heat and Mass Transfer*, to be published.

[13] Martellucci, A., Trucco, H., and Aguone, A., "Measurements of the Turbulent Near Wake of a Cone at Mach 6," *AIAA Journal*, Vol. 4, No. 3, March 1966, pp. 385–391.

[14] Scott, C. J. and Eckert, E. R. G., "Heat and Mass Exchange in the Supersonic Base Region," *AGARD Conference Proceedings, No. 4, Separated Flows*, Pt. 1, May 1966.

[15] Behrens, W. and Ko, D. T. S., "Experimental Stability Studies in Wakes of Two-Dimensional Slender Bodies at Hypersonic Speeds," *AIAA Journal*, Vol. 9, No. 5, May 1971, pp. 851–857.